

# Analysis of The $^{197}\text{Au}(p,d)^{196}\text{Au}$ Reaction at 68 MeV with Direct Reaction Model

S. A. Sultana

Bangladesh Open University, Gazipur 1705, Bangladesh

## Abstract

Double differential cross section for the  $^{197}\text{Au}(p,d)^{196}\text{Au}$  reaction has been studied here with 68 MeV protons for the  $30^\circ$ ,  $35^\circ$ ,  $45^\circ$  and  $60^\circ$  angles. Calculations of the spectra have been carried out here using the distorted wave Born approximation (DWBA) -based cross-sections and the asymmetric Lorentzian form strength response function having energy dependent spreading widths. The results of comparisons between the experimental and calculated spectra are described. Numerical values of the double differential cross sections are lower than experiment by approximately 10% or so.

**Keywords:** double differential cross section, (p,d), nuclear reactions, direct reaction model, DWBA analysis

## 1. Introduction

Generally, the spectrum of the emitted particles from one nucleon transfer reaction can be divided into three parts, because the mechanisms of this type of reaction are classified to three types, i.e. direct, pre-equilibrium and evaporation processes.

The evaporation and pre-equilibrium processes are analyzed with statistical models and present days some computer codes (GNASH, CASCADE, QMD) are available to calculate double differential cross sections [1-6]. However, the continuum spectrum in the direct reaction region is not possible to analyze easily.

From the above points of view, it is indispensable to develop a theoretical model which reproduces well the continuum spectra in the direct reaction regions. Therefore, an approach such as proposed by Lewis [7] is suggested to be employed, in parallel with the prediction models described by Crawley [8] and Gales et al. [9], therefore, is employed in the present analyses, based on the distorted wave born approximation (DWBA) and an asymmetric Lorentzian form strength function. Matoba et al. [10, 11] in agreement with Lewis [8] have advanced an analysis using an asymmetric Lorentzian shaped strength function having energy-dependent spreading widths and distorted wave born approximation (DWBA) cross sections. This model has been successfully applied for the (p,d) reactions [12-17], then applied for the (n,d) reaction [18-20] with a slight modification and demonstrate its reasonable ability.

In the present work, the continuum spectra for the  $^{197}\text{Au}(p,d)^{196}\text{Au}$  reaction have been analyzed by the same method of calculation. Here, the laboratory angles are  $30^\circ$ ,  $35^\circ$ ,  $45^\circ$  and  $60^\circ$  and the incident energy is 68 MeV. The experiments in the present work were carried out in the same way with exactly identical arrangements of the experiment given in section 2 and in details in ref. [21]. Earlier, another work [17] also was done at the same energy and for the same reaction but at different laboratory angles

$75^\circ$ ,  $90^\circ$  and  $120^\circ$  to make this method of calculation as a global one over a wide range of scattering angles. With the same method of calculation, the application of seniority scheme to the present model for odd target nucleus [i.e.  $^{197}\text{Au}(p,d)^{196}\text{Au}$ ] makes this model more feasible. The calculated results are compared here with the experimental ones.

## 2. Materials and Methods

### 2.1 Experimental Calculations

The experiments were performed at the ‘‘Takasaki Ion Accelerators for Advanced Radiation Application (TIARA)’’ facility of Japan Atomic Energy Research Institute (JAERI). A proton beam of 68 MeV from the AVF cyclotron was led to the HB-1 beam line.

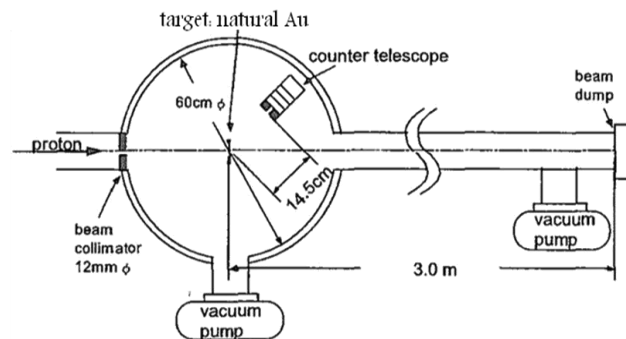


**Fig. 1:** Experimental setup of the HB-1 beam line

As illustrated in Fig. 1, the accelerated proton beam bombarded a thin target foil placed in the center of a 60 cm  $\phi$  scattering chamber installed in the HB 1 beam line. Energy distributions of light ions emitted from the target were measured using a  $\Delta E$ -E counter at  $25^\circ$ ,  $30^\circ$ ,  $35^\circ$ ,  $45^\circ$ ,  $60^\circ$ ,  $75^\circ$ ,  $90^\circ$ ,  $12^\circ$ , and  $150^\circ$  in the laboratory system. The counter telescope consisted of two thin silicon E-detectors (30  $\mu\text{m}$  and 500  $\mu\text{m}$  in thickness, respectively) and a CsI(Tl) E-detector (18 mm $\phi$  x 30 mm long) with photo-diode readout [21]. Energy distribution of light ions emitted from the target were measured using a  $\Delta E$ -E counter

telescope, which consisted of two thin silicon  $\Delta E$ -detectors and a CsI(Tl) E-detector with photo-diode readout. Details of the experimental procedure and the results have been reported in ref. [22].

## 2.2. Theoretical Calculations

In the present method, the theoretical calculations of the double differential cross-sections have been done by considering a direct reaction model as an incoherent sum of the direct reaction components, which are based on distorted wave born approximation (DWBA) predictions and expressed as below:

$$\frac{d^2\sigma}{d\Omega dE} = 2.30 \sum_{l,j} \left[ \frac{C^2 S_{l,j}(E)}{2j+1} \times \left( \frac{d\sigma}{d\Omega} \right)_{l,j}^{DW}(E) \right] \quad (1)$$

where  $d\sigma/d\Omega|_{l,j}^{DW}(E)$  is the cross-section calculated by a distorted wave born approximation (DWBA) code, DWUCK-4 (distorted wave born approximation, Zero range code) [23] and  $C^2 S_{l,j}(E)$ , the spectroscopic factor expressed as

$$C^2 S_{l,j}(E) = \left( \sum C^2 S_{l,j} \right) \times f_{l,j}(E). \quad (2)$$

where  $\sum C^2 S_{l,j}$  is the sum of the spectroscopic factors of all the predicted states and the distribution of strength function over the spectra is obtained by using an asymmetric Lorentzian function [11, 12, 24, 25]

$$f_{l,j}(E) = \frac{n_0}{2\pi} \frac{\Gamma(E)}{(|E - E_F| - E_{l,j})^2 + \Gamma^2(E)/4} \quad (3)$$

and

$$\int_0^{\alpha} f_{l,j}(E) dE = 1 \quad (4)$$

where  $n_0$  is the renormalization constant and  $E_F$  the Fermi energy. The Fermi energy can be calculated by using an empirical formula given in ref. [26]. The sums of spectroscopic factors and the centroid energies ( $E_{l,j}$ ) for  $J = l \pm \frac{1}{2}$  shell orbits have been estimated by using Bardeen-Cooper-Schrieffer (BCS theory) calculations. In these calculations, single particle energies required to calculate the centroid energy are calculated by the prescription of Bohr and Mottelson [27]. Spreading width ( $\Gamma$ ) is expressed by a function proposed by Brown and Rho [28] and by Mahaux and Sartor [24-25] as,

$$\Gamma(E) = \frac{\varepsilon_0(E - E_F)^2}{(E - E_F)^2 + E_0^2} + \frac{\varepsilon_1(E - E_F)^2}{(E - E_F)^2 + E_1^2} \quad (5)$$

Where,  $\varepsilon_0$ ,  $\varepsilon_1$ ,  $E_0$  and  $E_1$  are constants which express the effects of nuclear damping in the nucleus [10]. The estimated parameters [10] are

$$\begin{aligned} \varepsilon_0 &= 19.4 \text{ (MeV)}, & E_0 &= 18.4 \text{ (MeV)} \\ \varepsilon_1 &= 1.40 \text{ (MeV)}, & E_1 &= 1.60 \text{ (MeV)}. \end{aligned} \quad (6)$$

It should be mentioned here that the effects of the nuclear damping are felt in the continuum spectra of the double differential cross section much more in the lower energy regions than at higher energy. There is a close similarity between theory and experiment except that in the direct nuclear reactions the effects show dominance at lower energies. This is not unexpected.

The sum rule of the spectroscopic factors of nucleon orbits for  $T \pm \frac{1}{2}$  isospin states are estimated with a simple shell

model prescription [29]

$$\sum C^2 S_{l,j} = \begin{cases} \frac{n_n(l,j) - n_p(l,j)}{2T+1} & \text{for } T_c = T - \frac{1}{2} \\ \frac{n_p(l,j)}{2T+1} & \text{for } T_c = T + \frac{1}{2} \end{cases} \quad (7)$$

Here  $n_n(l, j)$  and  $n_p(l, j)$  are the numbers of neutrons and protons respectively for each  $l, j$  orbit and  $T$  is the isospin of the target nucleus.

## 3. Results and Discussion

Double differential cross-sections (DDXs) are calculated here for the  $^{197}\text{Au}(p,d)^{196}\text{Au}$  reaction at 68 MeV for the laboratory angles of  $30^\circ$ ,  $35^\circ$ ,  $45^\circ$  and  $60^\circ$  as shown in figs. 2-3. Experimental and theoretical results are given by the circles and lines respectively in Figs. 2 and 3. Theoretical results are in general agreement with experimental results and the discrepancies are not more than 10% for all optical model potentials.

Three global potentials were used here for protons, while for deuteron an adiabatic potential [29-31] based on the proton and neutron potentials were constructed for the DWUCK-4 calculations as shown in Table 1. The solid, dotted and short-long-dashed lines represent the DDX for Becchetti and Greenlees [29], Koning and Delaroche [30] and Menet et al. [31] potentials respectively.

Figs. 2 - 3 show that for  $30^\circ$ ,  $35^\circ$  and  $60^\circ$  laboratory angles, the theoretical values are fairly in good agreement with experimental ones with approximately 10% lower for all potentials [29-31]. For  $45^\circ$  laboratory angles, the theoretical result is in good agreement with the experimental one for the Koning and Delaroche [30] and Menet et al. [31] potentials.

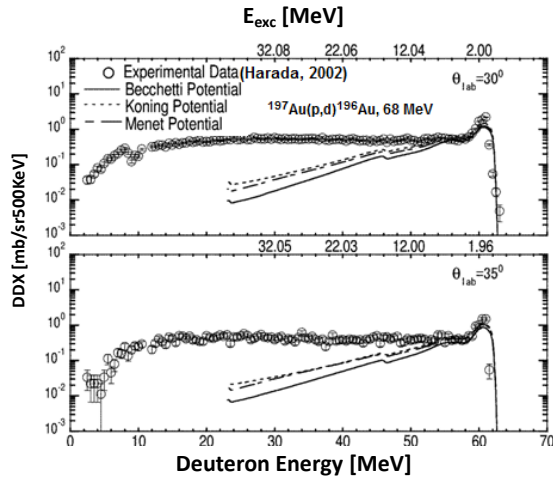


Fig. 2: Double differential cross sections for the  $^{197}\text{Au}(p,d)^{196}\text{Au}$  reaction at 68 MeV for  $30^\circ$  and  $35^\circ$  laboratory angles

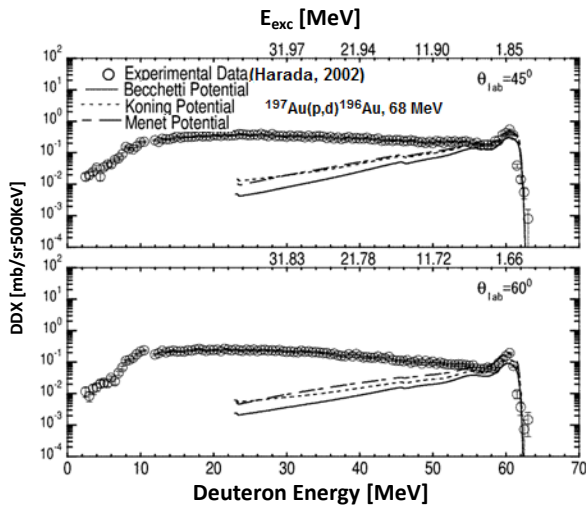


Fig. 3: Double differential cross sections for the  $^{197}\text{Au}(p,d)^{196}\text{Au}$  reaction at 68 MeV for  $45^\circ$  and  $60^\circ$  laboratory angles for Becchetti and Greenlees [29] potential.

Table 1: Optical model parameters used in the DWBA calculations for the  $^{127}\text{Au}(p,d)^{126}\text{Au}$  reaction at 68 MeV Becchetti and Greenlees potential [28]

Particle	V	r	a	r <sub>c</sub>	W <sub>v</sub>	W <sub>s</sub>	r'	a'	V <sub>so</sub>	r <sub>so</sub>	a <sub>so</sub>
	(MeV)	(fm)	(fm)	(fm)	(MeV)	(MeV)	(fm)	(fm)	(MeV)	(fm)	(fm)
Proton	42.42	1.17	0.75	1.25	12.26	0.00	1.32	0.65	6.20	1.01	0.75
Deuteron	a	1.17	0.78	1.25	b	b	1.29	0.65	6.20	1.06	0.75
Neutron	c	1.25	0.65								

$${}^aV = [110.3 - 0.64(E_d/2) + 0.4Z/A^{1/3}] \text{ MeV}$$

$${}^bW_v = [0.44(E_d/2) - 4.26] \text{ MeV}, W_s = [24.8 - 0.50(E_d/2)] \text{ MeV}, E_d \text{ is the deuteron kinetic energy and } {}^c\text{Well depth adjusted to fit the separation energy}$$

Koning and Delaroche potential [29]

Particle	V	R	a	r <sub>c</sub>	W <sub>v</sub>	W <sub>s</sub>	r'	a'	V <sub>so</sub>	r <sub>so</sub>	a <sub>so</sub>
	(MeV)	(fm)	(fm)	(fm)	(MeV)	(MeV)	(fm)	(fm)	(MeV)	(fm)	(fm)
Proton	30.63	1.23	0.65	1.22	6.72	4.96	1.25	0.51	4.85	1.07	0.59
Deuteron	a	1.23	0.65	1.22	a	a	1.25	0.57	a	1.07	0.59
Neutron	b	1.25	0.65								

<sup>a</sup>Adiabatic potentials with those of [29]

<sup>b</sup>Well depth adjusted to fit the separation energy

Menet potential [30]

Particle	V	R	A	r <sub>c</sub>	W <sub>v</sub>	W <sub>s</sub>	r'	a'	V <sub>so</sub>	r <sub>so</sub>	a <sub>so</sub>
	(MeV)	(fm)	(fm)	(fm)	(MeV)	(MeV)	(fm)	(fm)	(MeV)	(fm)	(fm)
Proton	45.60	1.16	0.75	1.25	7.32	3.87	1.37	0.40	6.04	1.06	0.75
Deuteron	a	1.16	0.75	1.25	b	b	1.37	c	6.04	1.06	0.75
Neutron	d	1.25	0.65								

$${}^aV = [99.8 - 0.44(E_d/2) + 0.4Z/A^{1/3}] \text{ MeV}$$

$${}^bW_v = [2.4 + 0.18(E_d/2)] \text{ MeV}, W_s = [8.40 - 0.10(E_d/2)] \text{ MeV}, E_d \text{ is the deuteron kinetic energy, } {}^c a' = 0.74 \cdot 0.008(E_d/2) + 1.0(N-Z)/2A \text{ and } {}^d\text{Well depth adjusted to fit the separation energy}$$

For all potentials nonlocality parameters and finite-range parameters are shown below:

	Nonlocality parameters	Finite-range parameter	λ= 25
proton	0.85fm	0.621	
neutron	0.85fm	0.621	
deuteron	0.54fm		

From the above discussion, we can find that the theoretical results are generally in good agreement with the experimental ones. The use of other optical model potentials may improve the theoretical results to fit the experimental ones.

Here, it should be noted that the calculated double differential cross sections agree with experimental data only above tens of MeV energy region, because our calculated energy spectrum regions are treated in the direct reaction scheme.

#### 4. Conclusion

The present work based on direct reaction model was carried out in the same line by Crawley [8] and Gales et al. [9]. Proton induced reaction on  $^{197}\text{Au}$  has been analyzed here with direct reaction model. Here, the incident energy is 68 MeV. The calculated DDXs show a good agreement with the experimental data both in magnitude and shape. Three global potentials are used for proton and deuteron in this theoretical model for the DWUCK-4 calculation for being confident about the theoretical method of DDX. We suggest here that using different optical model potentials may improve the result at forward angles.

### Acknowledgement

Author is grateful to Ikeda laboratory, Department of Applied Quantum Physics and Nuclear Engineering, Kyushu University, Japan for providing theoretical idea to advance this work and to Japan Atomic Energy Research Institute (JAERI), Japan for giving permission to measure the experimental data at the Takasaki Ion Accelerators for Advanced Radiation Application (TIARA) facility.

### References

1. C. Kalbach, Systematics of Continuum Angular Distributions: Extensions to Higher Energies, *Phys. Rev. C*, **37**, 2350 (1988).
2. H. W. Bertini, Low-Energy Intranuclear Cascade Calculation, *Phys. Rev.*, **131**, 1801 (1963).
3. H. W. Bertini, Intranuclear-Cascade Calculation of the Secondary Nucleon Spectra from Nucleon-Nucleus Interactions in The Energy Range 340 - 2900 MeV and Comparisons with Experiment, *Phys. Rev.*, **188**, 1711 (1969).
4. H. W. Bertini, Nonelastic Interactions of Nucleons and  $\pi$  Mesons with Complex Nuclei at Energies below 3 GeV, *Phys. Rev. C*, **6**, 660 (1972).
5. J. Aichelin, Quantum Molecular Dynamics-a Dynamical Microscopic  $n$ -Body Approach to Investigate Fragment Formation and The Nuclear Equation of State in Heavy Ion Collisions, *Phys. Rep.*, **202**, 233 (1991).
6. K. Niita, S. Chiba, T. Maruyama, Tomo. Maruyama, H. Takada, Takada, T. Fukahori, Y. Nakahara and A. Iwamoto, Analysis of the ( $N,xN'$ ) Reactions by Quantum Molecular Dynamics Plus Statistical Decay Model, *Phys. Rev. C*, **52**, 2620 (1995).
7. M. B. Lewis, Effects of Spreading Widths Upon The Direct Nuclear Reaction Continuum, *Phys. Rev. C*, **11**, 145 (1975).
8. G. M. Crawley, Highly Excited States in Nuclear Reactions, Proceedings of International Symposium, Osaka, (1980).
9. S. Gales, Ch. Stoyanov and A. I. Vdovin, Damping of High-Lying Single-Particle Modes in Heavy Nuclei, *Phys. Rep.*, **166**, 125 (1988).
10. M. Matoba, O. Iwamoto, Y. Uozumi, T. Sakae, N. Koori, H. Ohgaki, H. Kugimiya, H. Ijiri, T. Maki and M. Nakano, Fragmentation of Neutron-Hole Strengths in  $^{59}\text{Ni}$  Observed in the  $^{60}\text{Ni}(p,d)^{59}\text{Ni}$  Reaction at 65 MeV, *Nucl. Phys. A*, **581**, 21 (1995).
11. M. Matoba, K. Kurohmaru, O. Iwamoto, A. Nohtomi, Y. Uozumi, T. Sakae, N. Koori, H. Ohgaki, H. Ijiri, T. Maki, M. Nakano and H. M. Sen Gupta, ( $p,d$ ) Reaction on  $^{62}\text{Ni}$  at 65 MeV, *Phys. Rev. C*, **53**, 1792 (1996).
12. Syafarudin, F. Aramaki, G. Wakabayashi, Y. Uozumi, N. Ikeda, M. Matoba, K. Yamaguchi, T. Sakae, N. Koori and T. Maki, Continuum Spectra in One-nucleon Transfer Reactions- $(p, d)$  Reactions at Medium Energy Region, *J. Nucl. Sci. Technol.*, Suppl. 2, **1**, 377 (2002).
13. S. A. Sultana, D. Maki, G. Wakabayashi, Y. Uozumi, N. Ikeda, Syafarudin, F. Aramaki, T. Kawaguchi, M. Matoba and H.M. Sen Gupta, The  $^{96}\text{Mo}(p,d)^{95}\text{Mo}$  Reaction at 50 MeV, *Phys. Rev. C*, **70**, 034612(1) - 034612(15) (2004).
14. S. Hirowatari, Syafarudin, F. Aramaki, A. Nohtomi, G. Wakabayashi, Y. Uozumi, N. Ikeda, M. Matoba, Y. Aoki, K. Hirota, N. Okumura and T. Joh, Total-Reaction-Cross-Section Measurements for 30-60-MeV Protons and the Imaginary Optical Potential, *Nucl. Phys. A*, **714**, 3 (2003).
15. F. Aramaki, Syafarudin, G. Wakabayashi, Y. Uozumi, N. Ikeda, M. Matoba, T. Sakae and N. Koori,  $^{100}\text{Mo}(p,d)^{99}\text{Mo}$  reaction at 50 MeV and Direct Reaction Analysis, Proceedings of the 2002 Symposium on Nuclear Data, 178-182, JAERI-Conf. 2002-006.
16. S. A. Sultana, T. Kin, G. Wakabayashi, Y. Uozumi, N. Ikeda, Y. Watanabe and M. Matoba, Analysis of Continuum Spectra for Proton Induced Reactions on  $^{27}\text{Al}$ ,  $^{58}\text{Ni}$ ,  $^{90}\text{Zr}$ ,  $^{197}\text{Au}$  and  $^{209}\text{Bi}$  at 42 and 68 MeV Direct Reaction Model Analysis. Proceeding of the 2005 Symposium on Nuclear Data, 185-189, JAEA-Conf., 2006-009.
17. S. A. Sultana, D. R. Sarker, G. Wakabayashi, Y. Uozumi, N. Ikeda, Y. Watanabe and M. Matoba, Analysis of the  $^{197}\text{Au}(p,d)^{196}\text{Au}$  Reaction With Direct Reaction Model, *Nucl. Sci. Appl.*, **18** (1), 24-28 (2009).
18. S. A. Sultana, Syafarudin, F. Aramaki, D. Maki, G. Wakabayashi, Y. Uozumi, N. Ikeda, M. Matoba, Y. Watanabe and H. M. Sen Gupta, Analysis of Continuum Spectra of ( $n,d$ ) Reactions With Direct Reaction Model, Proceedings of the 2003 Symposium on Nuclear Data, 133 (JAERI-Conf 2004-005).
19. S. A. Sultana, Syafarudin, D. Maki, T. Kin, G. Wakabayashi, Y. Uozumi, N. Ikeda, Y. Watanabe, F. Aramaki, M. Matoba, T. Kawaguchi and H. M. Sen Gupta, Continuum Spectra Analysis of ( $p,d$ ) and ( $n,d$ ) Reactions on Bi in Several Tens of MeV Energy Region, Proceeding of 2004 Symposium on Nuclear Data of, 143 (JAERI-Conf., 2005-003).
20. S. A. Sultana, Continuum Spectra in One-nucleon Transfer Reaction-  $^{209}\text{Bi}(n,d)^{208}\text{Pb}$  Reaction,  $E_p = 41.0\text{-}53.5$  MeV, *Nucl. Sci. Appl.*, **15** (1), 53-57 (2006).
21. M. Harada, Y. Watanabe, Y. Tanaka, Y. Matsuoka, K. Shin, S. Meigo, H. Takada, T. Sasa, O. Iwamoto, T. Fukahori, S. Chiba and S. Tanaka, Light Charged-Particle Production in Proton-Induced Reactions on  $^{12}\text{C}$ ,  $^{27}\text{Al}$ ,  $^{58}\text{Ni}$ ,  $^{90}\text{Zr}$ ,  $^{197}\text{Au}$ , and  $^{209}\text{Bi}$  at 42 and 68 MeV, *J. Nucl. Sci. Technol.*, Suppl. 2, **1**, 393 (2002).
22. P. D. Kunz, DWBA code DWUCK- 4, University of Colorado (Unpublished).
23. C. Mahaux and R. Sartor, From Scattering to Very Deeply Bound Neutrons in  $^{208}\text{Pb}$ : Extended and Improved Moment Approaches, *Nucl. Phys. A*, **493**, 157 (1989).
24. C. Mahaux and R. Sartor, Single Particle Motion in Nuclei, *Adv. Nucl. Phys.*, **20**, 1 (1991).
25. K. Hisamochi, O. Iwamoto, A. Kisanuki, S. Budihardjo, S. Widodo, A. Nohtomi, Y. Uozumi, T. Sakae, M. Matoba, M. Nakano, T. Maki, S. Matsuki and N. Koori, Hole Strengths and Spreading Widths Observed in  $^{92}\text{Mo}(\bar{p}, d)^{91}\text{Mo}$  Reaction at 65 MeV, *Nucl. Phys. A*, **564**, 227 (1993).
26. A. Bohr and B. R. Mottelson, Nuclear Structure, W. A. Benjamin, INC., 1996, New York, Amsterdam, **1**, Appendix 2D.

27. G. E. Brown and M. Rho, The giant Gamow-Teller Resonance, Nucl. Phys. A, **372**, 397 (1981).
28. J. B. French and M. H. Macfarlane, Isobaric-Spin Splitting of Single-Particle Resonances, Nucl. Phys., **26**, 168 (1961).
29. F. D. Becchetti, and G.W. Greenlees, Nucleon-Nucleus Optical-Model Parameters,  $A > 40$ ,  $E < 50$  MeV, Phys. Rev., **182**, 1190 (1969).
30. A. J. Koning and J. P. Delaroche, Local and Global Nucleon Optical Models From 1 keV - 200 MeV, Nucl. Phys. A, **713**, 231 (2003).
31. J. J. H. Menet, E. E. Gross, J. J. Malanify and A. Zucker, Total-Reaction-Cross-Section Measurements for 30-60-MeV Protons and the Imaginary Optical Potential, Phys. Rev. C, **4**, 1114 (1971).